Thermodynamic properties of a superconductor interfaced with an altermagnet

Simran Chourasia [1,*] Aleksandr Svetogorov [2] Akashdeep Kamra [3,1] and Wolfgang Belzig [2,†]
[1]*Condensed Matter Physics Center (IFIMAC) and Departamento de Física Teórica de la Materia Condensada, Universidad Autónoma de Madrid, 28049 Madrid, Spain*
[2]*Fachbereich Physik, Universität Konstanz, 78457 Konstanz, Germany*
[3]*Department of Physics and Research Center OPTIMAS, Rheinland-Pfälzische Technische Universität Kaiserslautern-Landau, 67663 Kaiserslautern, Germany*

(Received 13 August 2024; revised 3 April 2025; accepted 16 May 2025; published 5 June 2025)

Recently introduced magnetic materials called altermagnets (AM) feature zero net magnetization but a momentum-dependent magnetic exchange field, which can have intriguing implications when combined with superconductivity. In our work, we use the quasiclassical framework to study the effects of such a material on a conventional superconductor (S) in an AM/S bilayer. We discuss the superconducting phase diagram and heat capacity of AM/S while making a comparison with a ferromagnet-superconductor bilayer. Furthermore, we examine the density of states and analyze the system's response to an external magnetic field. We illustrate the anisotropy of spin susceptibility and magnetization of AM/S by considering an external field in the in-plane and out-of-plane directions, thereby facilitating the scope of experimental detection and characterization of an AM in an AM/S hybrid system.

DOI: 10.1103/PhysRevB.111.224503

I. INTRODUCTION

The interplay of superconductivity and magnetism has been receiving significant attention in condensed matter physics for decades [1–5]. Nevertheless, the discoveries of novel hybrid materials and new experimental techniques constantly provide new interesting phenomena to study [6–12]. One of the latest additions to magnetic materials is a collinear symmetry-compensated antiferromagnet [13–15], for which the term "altermagnet" was introduced [16–19]. Recently, experimental evidence for that new type of magnetism has been reported [20]. Intrinsic anomalous Hall effect [21,22] and enhanced thermal transport [23] have also been predicted for these materials. The idea to combine this new type of material with superconductors emerged [24] right after theoretical predictions of altermagnets. Andreev reflection [25–28], Josephson effect [29–31], superconducting diode effect [32], topological superconductivity [33,34], magnetoelectric effect [35], spin-filtering effect [36], and inverse proximity effect using Bogoliubov–de Gennes formalism [37] were studied theoretically in altermagnet-superconductor (AM/S) hybrid structures. Intrinsic superconducting properties like finite-momentum superconductivity [38], allowed pairing symmetries [39], and topological superconductivity [40] have also been explored in altermagnets.

It is known that a spin-split band structure modifies the properties of a superconductor leading, e.g., to an inhomogenous superconducting state [41,42]. Spin splitting also modifies the superconducting transport in a variety of situations. This holds for magnetic barriers [43], magnetic insulators [44], as well as metals [1–3,45]. The manifestation of odd-frequency long-range triplet pairing has surged many experiments [6,46,47]. Spin effects can also be induced by an antiferromagnetic insulator [48–50] depending on the details of the interface coupling. Also, the proximity effect in antiferromagnets has been studied and led to the prediction of so-called Néel triplets [50–52].

In this work, we investigate the characteristics of a thin-film AM/S bilayer. Our objective is to study the magnetic inverse proximity effect that results in properties that can be experimentally measured and distinguish an AM/S bilayer from bilayers incorporating other magnetic materials. By formulating a minimal model of a bilayer of a thin superconductor in contact with an altermagnet in the quasiclassical framework, we find that the density of states of the superconductor in an AM/S bilayer has distinct features, and can lead to gapless superconductivity for a strong AM. We also study the superconducting phase diagram of the AM/S bilayer and find that the superconductor to normal metal (N) phase transition with increasing temperature is always second order. Further, we find that spin susceptibility and magnetization of AM/S in the presence of an external magnetic field show features that can serve as experimental signatures of d-wave altermagnetism.

II. MODEL

We consider a thin film of a conventional s-wave superconductor interfaced with an insulating altermagnet such that the thickness of the superconductor is much smaller than its

*Contact author: simran.chourasia@uam.es
†Contact author: wolfgang.belzig@uni-konstanz.de

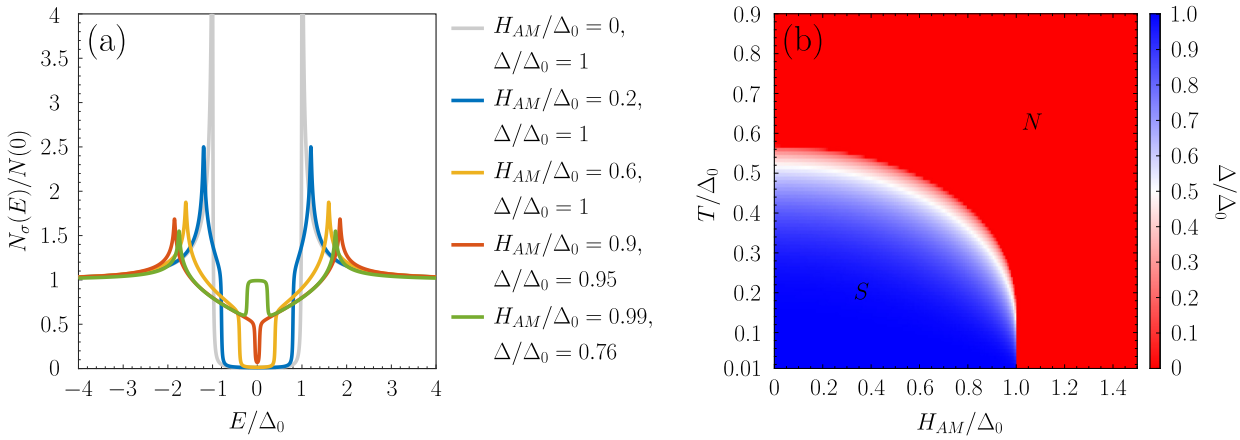

FIG. 1. (a) Superconductor's density of states (DOS) in an altermagnet-superconductor bilayer (AM/S) for different exchange strengths $H_{\rm AM}$ of the altermagnet is plotted for spin σ. Since the DOS of AM/S is found same for both spins, the curve for only spin-↑ quasiparticles is shown. Here, the DOS is plotted at temperature $T = 0.1\ \Delta_0$, $N(0)$ is the DOS of a normal metal for each spin, the gray curve is the DOS of an isolated superconductor, and Δ_0 is the superconducting order parameter of an isolated superconductor at zero temperature. (b) Phase diagram of AM/S as a plot of its superconducting order parameter Δ for different values of T and $H_{\rm AM}$, obtained irrespective of its initial guess value in the self-consistency calculation. The blue and red regions correspond to superconducting and normal states of the AM/S, respectively.

coherence length. We assume the AM affects the superconductor by imparting a momentum-dependent magnetic exchange field on the electrons of the superconductor [Fig. 2(a) inset]. Such spin- and momentum-dependent exchange field can be created by specular scattering off a magnetic insulator, which has been studied previously for the case of momentum dependence [53,54] or pure spin dependence [3,55,56]. Independent on detail, we therefore assume the presence of a momentum-dependent exchange field $\vec{H}_{\rm eff}(\hat{k})$ in the superconducting film that bears the symmetry of the altermagnetic magnetization. A microscopic derivation for the quasiclassical Green's function formalism follows from the analysis in [44,57] which we will not repeat here. The strength of the induced exchange field will vary depending on the interfacial coupling as well as the thickness of the superconducting film similar as discussed, e.g., in [58]. We emphasize here that the strength of the induced field is not equal to the internal exchange constants of the altermagnet, which is usually much larger. Hence, in the quasiclassical framework, the conduction electrons of the superconductor can be described by the following Eilenberger equation [59,60]:

$$\left[\omega_n(\hat{\boldsymbol{\sigma}}_{\mathbf{0}} \otimes \hat{\boldsymbol{\tau}}_z) + \check{\boldsymbol{\Delta}} - i\,\vec{H}_{\rm eff}(\hat{k}) \cdot \hat{\vec{\boldsymbol{\sigma}}} \otimes \hat{\boldsymbol{\tau}}_z,\ \check{\boldsymbol{g}}_{\omega_n}(\hat{k})\right] = \check{\mathbf{0}}, \quad (1)$$

where $\omega_n = (2n+1)\pi T$ is a Matsubara frequency for an integer n, T is the temperature, $\hat{k} = \cos(\phi)\hat{x} + \sin(\phi)\hat{y}$ is the two-dimensional unit vector along the crystal momentum $\vec{k}$ of the electron on the Fermi surface being described, and ϕ is the polar angle in the plane of the film. Matrices $\hat{\boldsymbol{\sigma}}_{\mathbf{0}}$ ($\hat{\boldsymbol{\tau}}_{\mathbf{0}}$) and $\hat{\boldsymbol{\sigma}}_{\boldsymbol{\alpha}}$ ($\hat{\boldsymbol{\tau}}_{\boldsymbol{\alpha}}$) with $\alpha \in \{x, y, z\}$ are identity and Pauli matrices in the spin (Nambu) space. We have neglected the derivative terms in Eq. (1) since we assume the thickness of the superconductor is much smaller than the coherence length. The superconducting pairing is described by $\check{\boldsymbol{\Delta}} = \Delta(\hat{\boldsymbol{\sigma}}_{\mathbf{0}} \otimes \hat{\boldsymbol{\tau}}_{\boldsymbol{x}})$, where Δ (assumed real) is the s-wave superconducting order parameter. The

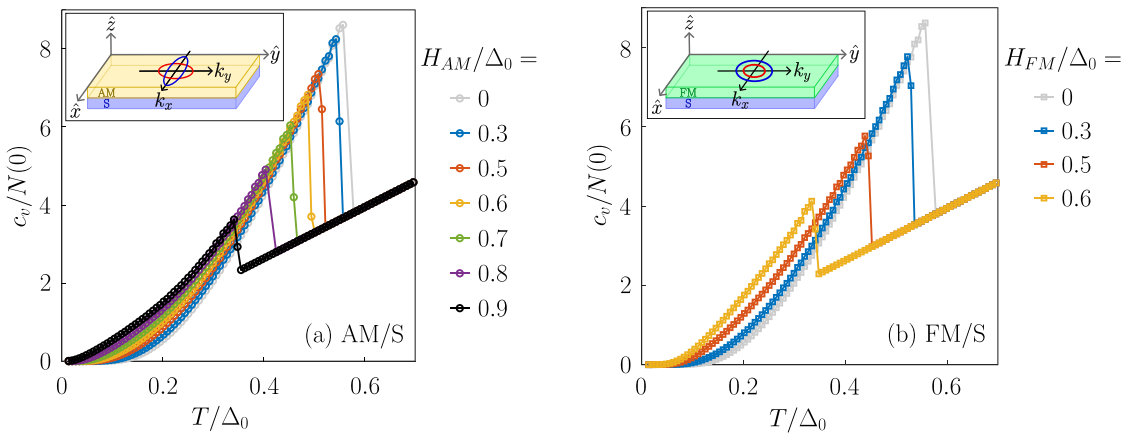

FIG. 2. Superconductor's temperature dependence of heat capacity per unit volume c_v in (a) altermagnet-superconductor (AM/S), and (b) ferromagnet-superconductor (FM/S) bilayers for different values of exchange field strengths. The insets show the schematic diagrams of the corresponding (a) AM/S and (b) FM/S bilayers with their normal-state Fermi surfaces of spin-up (blue) and -down (red) electrons drawn in the k_x-k_y plane.

electrons of the superconductor experience an effective d-wave exchange field, $\vec{H}_{\rm eff}(\hat{k}) \equiv \vec{H}_{\rm eff}(\phi) = H_{\rm AM}\cos(2\phi)\hat{z}$, due to its proximity to the AM [27,30]. This means the energies of spin-up and -down electrons with wave vector $\vec{k}$ get shifted by $\mp H_{\rm AM}\cos(2\phi)$. Here, $H_{\rm AM}$ is the amplitude of the altermagnetic exchange field and a larger $H_{\rm AM}$ means a stronger altermagnet. The quasiclassical Green's function $\check{\boldsymbol{g}}_{\omega_n}$, written in spin $\otimes$ Nambu space, contains all the relevant information of the system [61]. The commutator form of Eq. (1) ensures that $\check{\boldsymbol{g}}_{\omega_n}$ satisfies the normalization condition $\check{\boldsymbol{g}}_{\omega_n}\check{\boldsymbol{g}}_{\omega_n} = \check{\mathbf{1}}$ [60,62]. By satisfying $\mathrm{Tr}\,\check{\boldsymbol{g}}_{\omega_n} = 0$ and $\check{\boldsymbol{g}}_{\omega_n}\check{\boldsymbol{g}}_{\omega_n} = \check{\mathbf{1}}$, we get

$$\check{\boldsymbol{g}}_{\omega_n}(\hat{k}) = \begin{bmatrix} g_{\uparrow\uparrow,\omega_n} & if_{\uparrow\downarrow,\omega_n} & g_{\uparrow\downarrow,\omega_n} & if_{\uparrow\uparrow,\omega_n} \\ if^{\dagger}_{\downarrow\uparrow,\omega_n} & \bar{g}_{\downarrow\downarrow,\omega_n} & if^{\dagger}_{\downarrow\downarrow,\omega_n} & \bar{g}_{\downarrow\uparrow,\omega_n} \\ g_{\downarrow\uparrow,\omega_n} & if_{\downarrow\downarrow,\omega_n} & g_{\downarrow\downarrow,\omega_n} & if_{\downarrow\uparrow,\omega_n} \\ if^{\dagger}_{\uparrow\uparrow,\omega_n} & \bar{g}_{\uparrow\downarrow,\omega_n} & if^{\dagger}_{\uparrow\downarrow,\omega_n} & \bar{g}_{\uparrow\uparrow,\omega_n} \end{bmatrix}$$
$$= \frac{1}{2}(\hat{\boldsymbol{\sigma}}_{\mathbf{0}} + \hat{\boldsymbol{\sigma}}_z) \otimes \hat{\boldsymbol{g}}_{+,\omega_n}(\phi) + \frac{1}{2}(\hat{\boldsymbol{\sigma}}_{\mathbf{0}} - \hat{\boldsymbol{\sigma}}_z) \otimes \hat{\boldsymbol{g}}_{-,\omega_n}(\phi), \tag{2}$$

with

$$\hat{\boldsymbol{g}}_{\pm,\omega_n}(\phi) = \frac{[\omega_n \mp i\,H_{\rm AM}\cos(2\phi)]\hat{\boldsymbol{\tau}}_z + \Delta\hat{\boldsymbol{\tau}}_x}{\sqrt{[\omega_n \mp i\,H_{\rm AM}\cos(2\phi)]^2 + \Delta^2}}. \tag{3}$$

The order parameter Δ is calculated self-consistently as [61]

$$\Delta = i\pi\lambda T\sum_{n=0}^{N_0}\int_0^{2\pi}\frac{d\phi}{2\pi}[f_{\uparrow\downarrow,\omega_n} + f_{\downarrow\uparrow,\omega_n}], \tag{4}$$

where λ is the interaction constant, $N_0 = \lceil(\Omega_{\rm BCS}/\pi T - 1)/2\rceil$ depends on the BCS cutoff frequency $\Omega_{\rm BCS} = \frac{1}{2}\Delta_0\, e^{1/\lambda}$, and Δ_0 is the superconducting order parameter of an isolated superconductor at zero temperature.

Using this simple model, we describe how the AM modifies the properties of the superconductor in a thin-film AM/S, leaving questions about microscopic details like boundary conditions for future works. Since altermagnet candidates like MnTe [63], MnSe [64], and RuO_2 [65] have Néel temperatures much higher than the critical temperatures of conventional superconductors, the exchange field of the AM is assumed to remain constant for temperatures and magnetic fields varying within an order of Δ_0. Therefore, in our work, AM/S represents the superconducting layer of the AM/S bilayer. Although the exchange interaction responsible for AM's magnetic ordering is strong, the exchange field strength $H_{\rm AM}$ that gets imprinted on the superconductor should be weak enough to let the superconductivity survive in the AM/S bilayer. Our self-consistent calculation of Δ [Fig. 1(b)] shows that superconductivity survives only for $H_{\rm AM} < \Delta_0$, hence determining the regime for our calculations.

III. DOS, PHASE DIAGRAM AND HEAT CAPACITY

The density of states (DOS), $N_\sigma(E)$, of quasiparticles with energy E and spin σ in the AM/S can be calculated, by replacing $i\omega_n$ with $E + i\eta$ in Eq. (2) of $\check{\boldsymbol{g}}_{\omega_n}(\hat{k})$, as

$$\frac{N_\sigma(E)}{N(0)} = \int_0^{2\pi}\frac{d\phi}{2\pi}\mathrm{Re}[g_{\sigma\sigma,\omega_n}]_{i\omega_n\to E+i\eta}, \tag{5}$$

where η is a small positive number and $N(0)$ is the DOS of each spin in a normal metal at the Fermi surface. Figure 1(a) shows the DOS of AM/S for different strengths of altermagnetic exchange field. In AM/S, the change in the sign of $\vec{H}_{\rm eff}(\hat{k})$ with changing ϕ in the $\vec{k}$ space ensures that the DOS of spin-↑ and -↓ quasiparticles are same at each energy. We find that $N_\sigma(E)/N(0)$ has peaks at $E = \pm|\Delta + H_{\rm AM}|$ with logarithmic divergence and shoulderlike structures at $E = \pm|\Delta - H_{\rm AM}|$ for $H_{\rm AM} < \Delta$. For $H_{\rm AM} > \Delta$, the two shoulderlike structures of the DOS overlap with each other and lead to the closing of the gap in the spectrum, while retaining superconductivity, as in the case for the green curve in Fig. 1(a). The DOS evaluated for AM/S resembles the normalized total DOS, $[N_\uparrow(E) + N_\downarrow(E)]/2N(0)$, of the superconducting layer of an FM/S bilayer weighted averaged over the magnitude of exchange field varying from 0 to $H_{\rm AM}$.

In order to compare the superconducting phase diagram of AM/S with that of FM/S, we calculate Δ self-consistently and plot it, in Fig. 1(b), for different values of altermagnetic exchange strength $H_{\rm AM}$ and temperature T. We performed the self-consistent calculation of Δ starting with two different initial guess values $\Delta_{\rm initial} = 1.5\,\Delta_0$ and $\Delta_{\rm initial} = 0.01\,\Delta_0$. For both cases, we get the same solution for each value of $H_{\rm AM}$. Since the solution of self-consistent calculation converges to a local minima of the free energy near the initial guess value, this implies that the local minima near $\Delta_{\rm initial}/\Delta_0 = 1.5$ and 0.01 is the same and it corresponds to the global minima. This is different from the case of an FM/S, where the self-consistent calculation gives two different sets of solutions for $\Delta_{\rm initial}/\Delta_0 = 1.5$ and 0.01 (see Appendix) and a rigorous comparison between different free energies becomes essential to get the physical solution [66,67].

In the case of AM/S, the free energies of the metallic layer in its superconducting state ($F_{\rm S}$) and normal state ($F_{\rm N}$) for the critical altermagnetic amplitude $H_{{\rm AM},c}$, the highest value of $H_{\rm AM}$ for which the superconducting state is stable, at zero temperature are related as

$$F_N - F_S = N(0)\int_0^{2\pi}\frac{d\phi}{2\pi}[H_{{\rm AM},c}\cos(2\phi)]^2. \tag{6}$$

Comparing it to the BCS condensation energy $F_{\rm N} - F_{\rm S} = N(0)\Delta_0^2/2$ gives critical altermagnetic strength $H_{{\rm AM},c} = \Delta_0$ which is larger than the critical exchange field of an FM/S [68]. Furthermore, the unique solution of Δ in Fig. 1(b) obtained irrespective of the value of $\Delta_{\rm initial}$ from the self-consistent calculation satisfies the Pauli paramagnetic limit for AM/S, $H_{{\rm AM},c} = \Delta_0$, reaffirming that it corresponds to the stable solution. Therefore, the plot of self-consistent solution of Δ in Fig. 1(b) is a phase diagram of the AM/S obtained without accounting for Fulde-Ferrell-Larkin-Ovchinnikov (FFLO) states which could be stable in the presence of an altermagnetic exchange field [31,38]. From the phase diagram in Fig. 1(b), we observe that the S-N transition in AM/S with increasing temperature is a second-order transition at all values of $H_{\rm AM}$. This is unlike the phase diagram of an FM/S, where the S-N transition becomes first order for larger exchange field strengths [66].

We now consider the heat capacity per unit volume c_v, which is given by the expression [69]

$$\frac{c_v}{N(0)} = T\frac{d}{dT}\left[\frac{S_v}{N(0)}\right], \tag{7}$$

where S_v is the entropy per unit volume calculated as

$$S_v(T) = -\int dE[N_\uparrow(E) + N_\downarrow(E)]\{f(E)\ln f(E) + [1-f(E)]\ln[1-f(E)]\}, \tag{8}$$

and $f(E) = 1/(e^{E/T}+1)$ is the Fermi-Dirac distribution function with the Boltzmann constant set to 1. Figure 2 shows the temperature dependence of $c_v/N(0)$ for AM/S [Fig. 2(a)] and FM/S [Fig. 2(b)]. The insets of Figs. 2(a) and 2(b) show the schematic diagrams of AM/S and FM/S bilayers. The calculations for FM/S are done by substituting $\vec{H}_{\rm eff}(\hat{k}) = H_{\rm FM}\hat{z}$ in Eq. (1) and solving it. From Fig. 2(a), we observe that the $c_v/N(0)$ versus T curves of AM/S, for small T, gradually transition from exponential to nonexponential behavior with increasing value of $H_{\rm AM}$.

IV. RESPONSE TO AN EXTERNAL FIELD

Since AM/S under study has a unique d-wave spin-splitting field, its magnetic response to an external magnetic field can help in probing it experimentally. To incorporate an external magnetic field $\vec{h} = h_x\hat{x} + h_y\hat{y} + h_z\hat{z}$ applied on AM/S, we substitute $\vec{H}_{\rm eff}(\hat{k}) = \vec{H}_{\rm eff}(\phi) = \vec{h} + H_{\rm AM}\cos(2\phi)\hat{z}$ in Eq. (1), disregarding its orbital effects for simplicity as in [70,71]. We then solve it for $\check{g}_{\omega_n}(\hat{k})$ by satisfying $\mathrm{Tr}\,\check{g}_{\omega_n} = 0$ and $\check{g}_{\omega_n}\check{g}_{\omega_n} = \check{1}$, and using projector operators $\hat{P}_{\pm}(\phi)$ in the spin space for each $\vec{k}$ and find

$$\check{g}_{\omega_n}(\hat{k}) = \hat{P}_{+}(\phi)\otimes\hat{g}_{+,\omega_n}(\phi) + \hat{P}_{-,\omega_n}(\phi)\otimes\hat{g}_{-,\omega_n}(\phi), \tag{9}$$

where

$$\hat{g}_{\pm,\omega_n}(\phi) = \frac{[[\omega_n \mp i|\vec{H}_{\rm eff}(\phi)|]\hat{\tau}_z + \Delta\hat{\tau}_x]}{\sqrt{[\omega_n \mp i|\vec{H}_{\rm eff}(\phi)|]^2 + \Delta^2}} \tag{10}$$

and $\hat{P}_{\pm}(\phi) = [\hat{1} \pm \vec{n}(\phi)\cdot\hat{\vec{\sigma}}]/2$ with $\vec{n}(\phi)$ being the unit vector in direction of $\vec{H}_{\rm eff}(\phi)$. From $\check{g}_{\omega_n}$, the magnetization carried by the conduction electrons is calculated as [70–72]

$$M_\alpha = M_\alpha^N - \frac{i}{2}\pi N(0)T\sum_{\omega_n}\mathrm{Tr}\,\langle(\hat{\sigma}_\alpha\otimes\hat{\tau}_z)\check{g}_{\omega_n}(\hat{k})\rangle_{\hat{k}}, \tag{11}$$

where $\alpha \in \{x,y,z\}$, M_α is the magnetization along $\hat{\alpha}$ axis, $\langle\ldots\rangle_{\hat{k}}$ means averaging over all directions in the $\vec{k}$ space, and $M_\alpha^N = \chi^N\langle\vec{H}_{\rm eff}(\phi)\rangle_{\hat{k}}\cdot\hat{\alpha} = \chi^N h_\alpha$ is the magnetization of the normal metal in an AM/N bilayer, and $\chi^{\rm N} = 2N(0)$ is the linear spin susceptibility of the normal state.

The magnetization is found to be independent of the direction of $\vec{h}$ in the x-y plane [Fig. 2(a) inset] of AM/S. However, it has a different dependence on the z component of $\vec{h}$. We, therefore, study two cases: (a) when the external field is applied in the x-y plane (in plane) by choosing $\vec{h} = h\hat{x}$, and (b) when the external field is applied out of plane as $\vec{h} = h\hat{z}$. From now on, $\parallel$ represents that the applied field is in plane and $\perp$ represents that the applied field is out of plane.

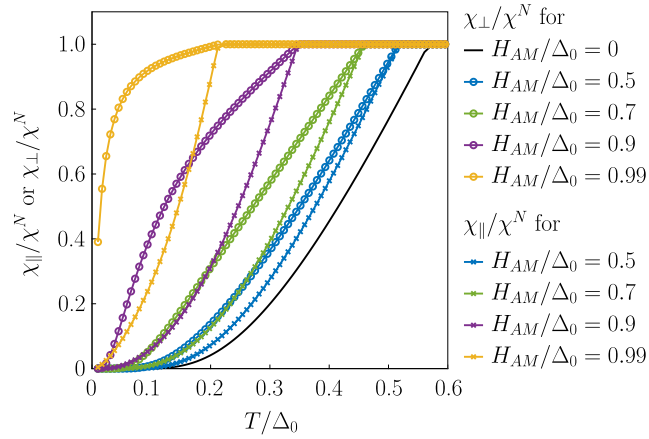

FIG. 3. Superconductor's linear susceptibility in an AM/S bilayer is plotted as a function of temperature T for different values of altermagnetic exchange strength $H_{\rm AM}$. The curves with "x" and "o" markers correspond to the in-plane ($\chi_\parallel$) and out-of-plane ($\chi_\perp$) susceptibilities, respectively. Curves of the same colors correspond to the same AM/S parameters. Here, an applied field of magnitude $h = 0.01\Delta_0$ is used for the calculation and $\chi^{\rm N}$ is the normal-state susceptibility.

We first study the linear susceptibility as it can be useful in characterizing the pairing symmetry of the AM/S. The in-plane (out-of-plane) linear susceptibility $\chi_{\parallel(\perp)}$ of the superconducting layer of AM/S can be calculated from its magnetization $M_{x(z)}^{\parallel(\perp)}$ in response to a very small magnetic field applied along $\hat{x}$ ($\hat{z}$) direction as

$$\frac{\chi_{\parallel(\perp)}}{\chi^{\rm N}} = \lim_{h\to 0}\frac{M_{x(z)}^{\parallel(\perp)}}{M_{x(z)}^{{\rm N},\parallel(\perp)}}, \tag{12}$$

where $M_{x(z)}^{{\rm N},\parallel(\perp)}$ is the magnetization along $\hat{x}$ ($\hat{z}$) for an applied in-plane (out-of-plane) magnetic field in an AM/N. The temperature dependence of linear susceptibilities of AM/S is shown in Fig. 3, where it is clear that $\chi_\perp/\chi^{\rm N} \geqslant \chi_\parallel/\chi^{\rm N}$ at all temperatures. The in-plane susceptibility curves ($\chi_\parallel/\chi^{\rm N}$) are convex and similar in shape to that of an isolated superconductor (black curve in Fig. 3). Whereas the curves for the out-of-plane case ($\chi_\perp/\chi^{\rm N}$), get modified from convex to roughly linear to highly concave curves with increasing $H_{\rm AM}$.

Since the intrinsic $\vec{k}$-dependent exchange field of the AM/S is in the out-of-plane direction, it does not have a direct effect on the in-plane susceptibility. However, AM's exchange field modifies the DOS of the superconductor in its proximity, leading to an indirect quantitative effect on $\chi_\parallel/\chi^{\rm N}$. This means that the $\chi_\parallel/\chi^{\rm N}$ curves for a superconductor get modified quantitatively and not qualitatively on interfacing it with an AM. On the other hand, an external field in the out-of-plane direction modifies the d-wave intrinsic exchange field of the superconducting layer of AM/S such that the electrons experience stronger spin splitting in the k_x direction and a reduced magnitude in the k_y direction. Applying the external field along $\hat{z}$ is therefore different in nature and allows one to probe the d-wave exchange field of the AM/S.

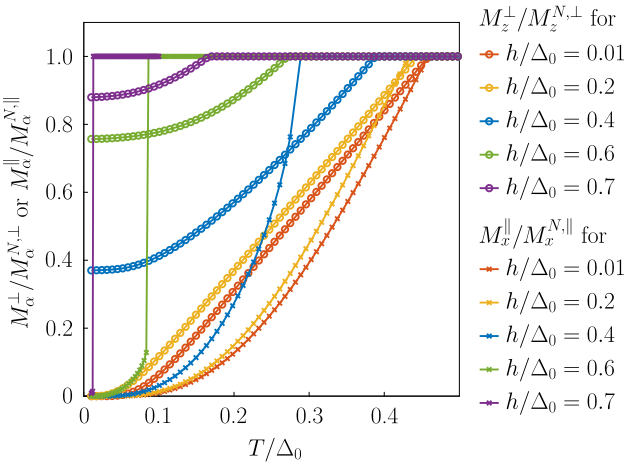

FIG. 4. Superconductor's magnetization in an AM/S bilayer normalized by its normal-state value $M_\alpha^{\perp}/M_\alpha^{\mathrm{N},\perp}$ ($M_\alpha^{\parallel}/M_\alpha^{\mathrm{N},\parallel}$) for $\alpha \in \{x, y, z\}$, is plotted as a function of temperature T when an external magnetic field $\vec{h} = h\hat{z}$ ($\vec{h} = h\hat{x}$) is applied out of plane (in plane). Here, the altermagnetic exchange strength is taken to be $H_{\mathrm{AM}} = 0.7\Delta_0$, and only the nonzero components of magnetization are plotted.

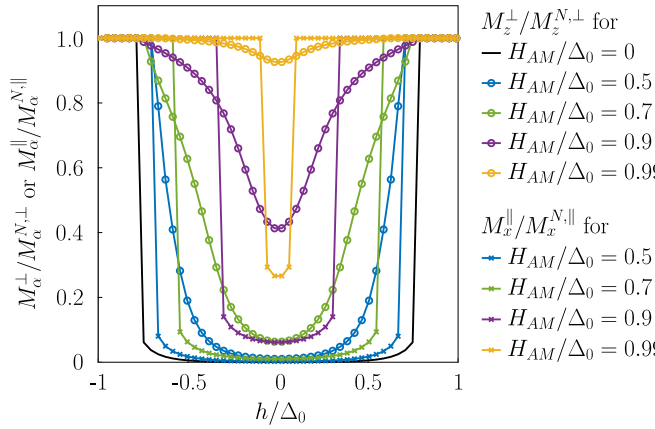

FIG. 5. Superconductor's magnetization in an AM/S bilayer normalized by its a normal-state value, $M_\alpha^{\perp}/M_\alpha^{\mathrm{N},\perp}$ ($M_\alpha^{\parallel}/M_\alpha^{\mathrm{N},\parallel}$) for $\alpha \in \{x, y, z\}$, is plotted as a function of h, the magnitude of applied field $\vec{h} = h\hat{z}$ ($\vec{h} = h\hat{x}$) in the out-of-plane (in-plane) direction. Here, only the nonzero components of magnetization are plotted, and the temperature is $T = 0.1\Delta_0$. Close to the transition, the physical behavior may differ from the curves shown both here and in Fig. 4 due to considerations of the free energy in presence of uniform exchange field [66].

Figure 4 shows the temperature dependence of the superconductor's magnetization in an AM/S bilayer for different strengths of applied magnetic fields in the in-plane and out-of-plane directions. We observe that the magnetization $M_z^{\perp}/M_z^{\mathrm{N},\perp}$, when the applied field is out of plane, behaves similar to the linear susceptibility $\chi_{\perp}/\chi^{\mathrm{N}}$ (red curve with circle markers in Fig. 4) for a weak applied field, whereas it becomes nonzero at zero temperature for stronger fields. In presence of an out-of-plane applied field, the effective spin-splitting field is $\vec{H}_{\mathrm{eff}}(\phi) = [H_{\mathrm{AM}}\cos(2\phi) + h]\hat{z}$. When $H_{\mathrm{AM}} + h > \Delta_0$, the superconducting gap in the DOS [Fig. 1(a)] closes at zero temperature making quasiparticles available for magnetization. However, one can see that it is possible to have $|\vec{H}_{\mathrm{eff}}(\phi)| = \sqrt{H_{\mathrm{AM}}^2\cos^2(2\phi) + h^2} < \Delta_0$ (for all ϕ) for the same magnitude of the external field if it is in plane, which provides a qualitative difference in the magnetization behavior at low temperatures (see the green and violet lines of Fig. 4).

The magnetization $M_x^{\parallel}/M_x^{\mathrm{N},\parallel}$ curves for an in-plane magnetic field in Fig. 4 behave similar to that of an isolated superconductor with a modified superconducting critical temperature T_c. This is because the AM's intrinsic exchange field is out of plane and does not affect the in-plane magnetization.

The suppression of T_c of an AM/S is stronger when the magnetic field is applied in plane (Fig. 4). This is because the magnetic field gets partially (in a part of the $\vec{k}$ space) screened by the AM's intrinsic exchange field when applied out of plane, which does not happen in the in-plane case.

Figure 5 shows the magnetization of the superconductor in an AM/S bilayer as a function of in-plane and out-of-plane applied magnetic field at $T = 0.1\Delta_0$. In AM/S, the superconductor's magnetization $M_x^{\parallel}/M_x^{\mathrm{N},\parallel}$ in an applied in-plane magnetic field behaves similar to an isolated superconductor (black curve in Fig. 5). This is consistent with Figs. 3 and 4 which show that the AM does not have a direct effect on the superconductor's in-plane magnetization. However, the out-of-plane magnetization $M_z^{\perp}/M_z^{\mathrm{N},\perp}$ curve shows a very different trend as the out-of-plane applied field interferes with the d-wave nature of the intrinsic exchange field of AM/S. Also, the magnetization in the out-of-plane case is always larger than that in the in-plane case. This is because the maximum magnitude of the exchange field in the out-of-plane case $H_{\mathrm{AM}} + h$ is larger than that in the in-plane case $\sqrt{H_{\mathrm{AM}}^2 + h^2}$.

V. SUMMARY

In summary, we applied the quasiclassical Green's function approach to study a few properties of the AM/S bilayer. To this end, we calculated the DOS for such a system and demonstrated that it resembles the DOS of an FM/S bilayer averaged over the varying exchange field. We plotted the specific heat and the phase diagram, which differs from the ferromagnetic case by the absence of first-order transitions for higher exchange fields. Another feature that can differentiate and help characterize such a bilayer is its response to an external magnetic field. The spin susceptibility shows strong anisotropy, specifically in-plane susceptibility being qualitatively similar to the case of an isolated superconductor, while the out-of-plane field reveals the d-wave nature of the magnetism in AM. These results are essential to understand the properties of new hybrid materials constituting AMs and superconductors. Moreover, the unique features of the AM/S bilayer should allow for experimental verification if the hybrid structure does possess both altermagnetic and superconducting properties or if the proximity effect suppresses either of them.

ACKNOWLEDGMENTS

S.C. and A.K. acknowledge financial support from the Spanish Ministry for Science and Innovation–AEI Grant No. CEX2018-000805-M (through the "Maria de Maeztu"

Programme for Units of Excellence in R&D) and Grant No. RYC2021-031063-I funded by MCIN/AEI/10.13039/501100011033 and "European Union Next Generation EU/PRTR." S.C. also acknowledges Spanish MICINN (Grants No. PID2019-109539GB-C43, No. TED2021-131323B-I00, and No. PID2022-141712NB-C21), Generalitat Valenciana through Programa Prometeo (2021/017), the computational resources provided by Centro de Computación Científica of the Universidad Autónoma de Madrid, and Grant No. PREP2022-000250 funded by MICIU/AEI/10.13039/501100011033 and by ESF+. A.S. and W.B. acknowledge support by the Deutsche Forschungsgemeinschaft (DFG; German Research Foundation) through SFB 1432 (Project ID No. 425217212) and and SPP2244 (Project ID No. 417034116).

APPENDIX: SELF-CONSISTENT SOLUTIONS OF Δ IN FM/S

In this Appendix, we discuss the case of a thin-film FM/S bilayer. We solve Eq. (1) of the main text for $\vec{H}_{\rm eff}(\hat{k}) = H_{\rm FM}\hat{z}$ to calculate Δ self-consistently using Eq. (4), where $H_{\rm FM}$ is the magnitude of uniform exchange field imparted by the insulating FM on the electrons of the superconductor. The set of solutions obtained by calculating Δ self-consistently starting with an initial guess of $\Delta_{\rm initial}/\Delta_0 = 1.5$ is plotted in Fig. 6. When the self-consistent calculation is started with an initial guess of $\Delta_{\rm initial}/\Delta_0 = 0.01$, the solutions are different. A comparison between these two solutions is shown in the inset of Fig. 6 by plotting T versus the minimum value of $H_{\rm FM}$, $H_{{\rm FM},c}$, at which the solution vanishes for a given T and $\Delta_{\rm initial}$. The self-consistency field converges to different set of solutions for different values of $\Delta_{\rm initial}$ because there are multiple local minima of the free energy and the solution converges to the nearest local minima. One needs to compare the free energies at all these local minima and determine the global minima which will correspond to the physical solution of Δ. In Fig. 6, the color changes from blue to white to red with increasing temperature for lower values of $H_{\rm FM}$. The absence of the white region at higher $H_{\rm FM}$ values indicates first-order S-N transition. A similar behavior where the S-N transition with increasing temperature is second-order for smaller values of $H_{\rm FM}$ and first-order for larger $H_{\rm FM}$ is observed in the phase diagram of an FM/S bilayer [66,67]. However, in the case of AM/S, S-N transition with increasing temperature always has the white region indicating second-order transition for all values of $H_{\rm AM}$ [Fig. 1(b)].

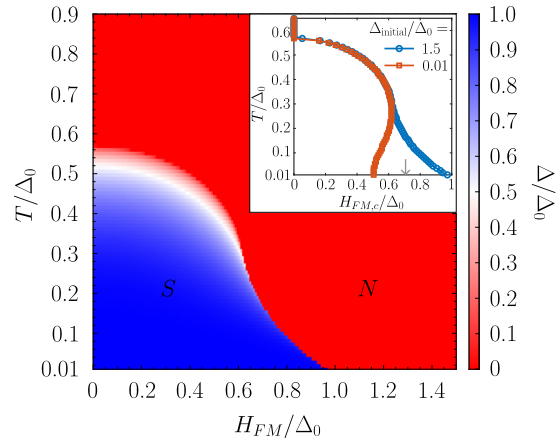

FIG. 6. Solution of order parameter Δ of a superconductor proximitized with ferromagnet, calculated self-consistently starting with an initial guess value $\Delta_{\rm initial} = 1.5\,\Delta_0$, for different values of temperature T and ferromagnetic exchange field $H_{\rm FM}$. Inset: A plot of T versus the minimum value of $H_{\rm FM}$, $H_{{\rm FM},c}$, at which the self-consistent solution of Δ vanishes. It shows the two solutions of $H_{{\rm FM},c}$ obtained from the self-consistent calculation of Δ starting with two different initial guess values $\Delta_{\rm initial}$. The physical solution of Δ and $H_{{\rm FM},c}$ are obtained by minimizing the free energies [66]. For example, at zero temperature $H_{{\rm FM},c} = \Delta_0/\sqrt{2}$ as indicated in the plot by an arrow.

[1] F. S. Bergeret, A. F. Volkov, and K. B. Efetov, Odd triplet superconductivity and related phenomena in superconductor-ferromagnet structures, Rev. Mod. Phys. **77**, 1321 (2005).

[2] A. I. Buzdin, Proximity effects in superconductor-ferromagnet heterostructures, Rev. Mod. Phys. **77**, 935 (2005).

[3] M. Eschrig and T. Löfwander, Triplet supercurrents in clean and disordered half-metallic ferromagnets, Nat. Phys. **4**, 138 (2008).

[4] J. Linder and J. W. A. Robinson, Superconducting spintronics, Nat. Phys. **11**, 307 (2015).

[5] F. S. Bergeret, M. Silaev, P. Virtanen, and T. T. Heikkilä, *Colloquium*: Nonequilibrium effects in superconductors with a spin-splitting field, Rev. Mod. Phys. **90**, 041001 (2018).

[6] T. S. Khaire, M. A. Khasawneh, W. P. Pratt, and N. O. Birge, Observation of spin-triplet superconductivity in Co-based Josephson junctions, Phys. Rev. Lett. **104**, 137002 (2010).

[7] C.-T. Wu, O. T. Valls, and K. Halterman, Reentrant superconducting phase in conical-ferromagnet–superconductor nanostructures, Phys. Rev. Lett. **108**, 117005 (2012).

[8] B. Baek, W. H. Rippard, S. P. Benz, S. E. Russek, and P. D. Dresselhaus, Hybrid superconducting-magnetic memory device using competing order parameters, Nat. Commun. **5**, 3888 (2014).

[9] K.-R. Jeon, C. Ciccarelli, A. J. Ferguson, H. Kurebayashi, L. F. Cohen, X. Montiel, M. Eschrig, J. W. A. Robinson, and M. G. Blamire, Enhanced spin pumping into superconductors provides evidence for superconducting pure spin currents, Nat. Mater. **17**, 499 (2018).

[10] S. Diesch, P. Machon, M. Wolz, C. Sürgers, D. Beckmann, W. Belzig, and E. Scheer, Creation of equal-spin triplet superconductivity at the Al/EuS interface, Nat. Commun. **9**, 5248 (2018).

[11] K.-R. Jeon, X. Montiel, S. Komori, C. Ciccarelli, J. Haigh, H. Kurebayashi, L. F. Cohen, A. K. Chan, K. D. Stenning, C.-M. Lee, M. Eschrig, M. G. Blamire, and J. W. A. Robinson, Tunable pure spin supercurrents and the demonstration of their gateability in a spin-wave device, Phys. Rev. X **10**, 031020 (2020).

[12] F. Chiodi, J. D. S. Witt, R. G. J. Smits, L. Qu, G. B. Halász, C.-T. Wu, O. T. Valls, K. Halterman, J. W. A. Robinson, and M. G. Blamire, Supra-oscillatory critical temperature dependence of Nb-Ho bilayers, Europhys. Lett. **101**, 37002 (2013).

[13] S. Hayami, Y. Yanagi, and H. Kusunose, Momentum-dependent spin splitting by collinear antiferromagnetic ordering, J. Phys. Soc. Jpn. **88**, 123702 (2019).

[14] L.-D. Yuan, Z. Wang, J.-W. Luo, E. I. Rashba, and A. Zunger, Giant momentum-dependent spin splitting in centrosymmetric low-z antiferromagnets, Phys. Rev. B **102**, 014422 (2020).

[15] I. I. Mazin, K. Koepernik, M. D. Johannes, R. González-Hernández, and L. Šmejkal, Prediction of unconventional magnetism in doped $FeSb_2$, Proc. Natl. Acad. Sci. USA **118**, e2108924118 (2021).

[16] L. Šmejkal, J. Sinova, and T. Jungwirth, Emerging research landscape of altermagnetism, Phys. Rev. X **12**, 040501 (2022).

[17] L. Šmejkal, J. Sinova, and T. Jungwirth, Beyond conventional ferromagnetism and antiferromagnetism: A phase with nonrelativistic spin and crystal rotation symmetry, Phys. Rev. X **12**, 031042 (2022).

[18] I. Mazin and The PRX Editors, Editorial: Altermagnetism—a new punch line of fundamental magnetism, Phys. Rev. X **12**, 040002 (2022).

[19] I. Mazin, Altermagnetism then and now, Physics **17**, 4 (2024).

[20] S. Lee, S. Lee, S. Jung, J. Jung, D. Kim, Y. Lee, B. Seok, J. Kim, B. G. Park, L. Šmejkal, C.-J. Kang, and C. Kim, Broken Kramers degeneracy in altermagnetic MnTe, Phys. Rev. Lett. **132**, 036702 (2024).

[21] L. Attias, A. Levchenko, and M. Khodas, Intrinsic anomalous Hall effect in altermagnets, Phys. Rev. B **110**, 094425 (2024).

[22] V. P. Mineev, Altermagnetic and noncentrosymmetric metals, JETP Lett. **121**, 421 (2025).

[23] X. Zhou, W. Feng, R.-W. Zhang, L. Šmejkal, J. Sinova, Y. Mokrousov, and Y. Yao, Crystal thermal transport in altermagnetic RuO_2, Phys. Rev. Lett. **132**, 056701 (2024).

[24] I. I. Mazin, Notes on altermagnetism and superconductivity, arXiv:2203.05000.

[25] C. Sun, A. Brataas, and J. Linder, Andreev reflection in altermagnets, Phys. Rev. B **108**, 054511 (2023).

[26] M. Wei, L. Xiang, F. Xu, L. Zhang, G. Tang, and J. Wang, Gapless superconducting state and mirage gap in altermagnets, Phys. Rev. B **109**, L201404 (2024).

[27] M. Papaj, Andreev reflection at the altermagnet-superconductor interface, Phys. Rev. B **108**, L060508 (2023).

[28] Y. Nagae, A. P. Schnyder, and S. Ikegaya, Spin-polarized specular Andreev reflections in altermagnets, Phys. Rev. B **111**, L100507 (2025).

[29] J. A. Ouassou, A. Brataas, and J. Linder, dc Josephson effect in altermagnets, Phys. Rev. Lett. **131**, 076003 (2023).

[30] C. W. J. Beenakker and T. Vakhtel, Phase-shifted Andreev levels in an altermagnet Josephson junction, Phys. Rev. B **108**, 075425 (2023).

[31] S.-B. Zhang, L.-H. Hu, and T. Neupert, Finite-momentum Cooper pairing in proximitized altermagnets, Nat. Commun. **15**, 1801 (2024).

[32] S. Banerjee and M. S. Scheurer, Altermagnetic superconducting diode effect, Phys. Rev. B **110**, 024503 (2024).

[33] Y.-X. Li and C.-C. Liu, Majorana corner modes and tunable patterns in an altermagnet heterostructure, Phys. Rev. B **108**, 205410 (2023).

[34] S. A. A. Ghorashi, T. L. Hughes, and J. Cano, Altermagnetic routes to Majorana modes in zero net magnetization, Phys. Rev. Lett. **133**, 106601 (2024).

[35] A. A. Zyuzin, Magnetoelectric effect in superconductors with d-wave magnetization, Phys. Rev. B **109**, L220505 (2024).

[36] H. G. Giil, B. Brekke, J. Linder, and A. Brataas, Quasiclassical theory of superconducting spin-splitter effects and spin-filtering via altermagnets, Phys. Rev. B **110**, L140506 (2024).

[37] H. G. Giil and J. Linder, Superconductor-altermagnet memory functionality without stray fields, Phys. Rev. B **109**, 134511 (2024).

[38] D. Chakraborty and A. M. Black-Schaffer, Zero-field finite-momentum and field-induced superconductivity in altermagnets, Phys. Rev. B **110**, L060508 (2024).

[39] D. Chakraborty and A. M. Black-Schaffer, Constraints on superconducting pairing in altermagnets, arXiv:2408.03999.

[40] D. Zhu, Z.-Y. Zhuang, Z. Wu, and Z. Yan, Topological superconductivity in two-dimensional altermagnetic metals, Phys. Rev. B **108**, 184505 (2023).

[41] P. Fulde and R. A. Ferrell, Superconductivity in a strong spin-exchange field, Phys. Rev. **135**, A550 (1964).

[42] A. I. Larkin and Yu. N. Ovchinnikov, Inhomogeneous state of superconductors, ZhETF **47**, 1136 (1964) [Sov. Phys. JETP **20**, 762 (1965)].

[43] P. M. Tedrow, J. E. Tkaczyk, and A. Kumar, Spin-polarized electron tunneling study of an artificially layered superconductor with internal magnetic field: EuO-Al, Phys. Rev. Lett. **56**, 1746 (1986).

[44] A. Millis, D. Rainer, and J. A. Sauls, Quasiclassical theory of superconductivity near magnetically active interfaces, Phys. Rev. B **38**, 4504 (1988).

[45] L.N. Bulaevskii, A.I. Buzdin, and S.V. Panjukov, The oscillation dependence of the critical current on the exchange field of ferromagnetic metals (F) in josephson junction SFS, Solid State Commun. **44**, 539 (1982).

[46] R. S. Keizer, S. T. B. Goennenwein, T. M. Klapwijk, G. Miao, G. Xiao, and A. Gupta, A spin triplet supercurrent through the half-metallic ferromagnet CrO_2, Nature (London) **439**, 825 (2006).

[47] J. W. A. Robinson, J. D. S. Witt, and M. G. Blamire, Controlled injection of spin-triplet supercurrents into a strong ferromagnet, Science **329**, 59 (2010).

[48] M. Hübener, D. Tikhonov, I. A. Garifullin, K. Westerholt, and H. Zabel, The antiferromagnet/superconductor proximity effect in Cr/V/Cr trilayers, J. Phys.: Condens. Matter **14**, 8687 (2002).

[49] A. Kamra, A. Rezaei, and W. Belzig, Spin splitting induced in a superconductor by an antiferromagnetic insulator, Phys. Rev. Lett. **121**, 247702 (2018).

[50] L. J. Kamra, S. Chourasia, G. A. Bobkov, V. M. Gordeeva, I. V. Bobkova, and A. Kamra, Complete T_c suppression and Néel triplets mediated exchange in antiferromagnet-superconductor-antiferromagnet trilayers, Phys. Rev. B **108**, 144506 (2023).

[51] G. A. Bobkov, I. V. Bobkova, A. M. Bobkov, and A. Kamra, Néel proximity effect at antiferromagnet/superconductor interfaces, Phys. Rev. B **106**, 144512 (2022).

[52] S. Chourasia, L. J. Kamra, I. V. Bobkova, and A. Kamra, Generation of spin-triplet Cooper pairs via a canted antiferromagnet, Phys. Rev. B **108**, 064515 (2023).

[53] C. Bruder, Andreev scattering in anisotropic superconductors, Phys. Rev. B **41**, 4017 (1990).

[54] M. Eschrig, Distribution functions in nonequilibrium theory of superconductivity and Andreev spectroscopy in unconventional superconductors, Phys. Rev. B **61**, 9061 (2000).

[55] A. Cottet, B. Douçot, and W. Belzig, Finite frequency noise of a superconductor-ferromagnet quantum point contact, Phys. Rev. Lett. **101**, 257001 (2008).

[56] A. Cottet and W. Belzig, Conductance and current noise of a superconductor/ferromagnet quantum point contact, Phys. Rev. B **77**, 064517 (2008).

[57] T. Tokuyasu, J. A. Sauls, and D. Rainer, Proximity effect of a ferromagnetic insulator in contact with a superconductor, Phys. Rev. B **38**, 8823 (1988).

[58] P. Machon, M. Eschrig, and W. Belzig, Nonlocal thermoelectric effects and nonlocal onsager relations in a three-terminal proximity-coupled superconductor-ferromagnet device, Phys. Rev. Lett. **110**, 047002 (2013).

[59] G. Eilenberger, Transformation of Gorkov's equation for type ii superconductors into transport-like equations, Z. Phys. **214**, 195 (1968).

[60] A. I. Larkin and Y. N. Ovchinnikov, Quasiclassical method in the theory of superconductivity, ZhETF **55**, 2262 (1968) [Sov. Phys.–JETP **28**, 1200 (1969)].

[61] N. B. Kopnin, *Theory of Nonequilibrium Superconductivity* (Clarendon, Oxford, 2001).

[62] U. Eckern and A. Schmid, Quasiclassical Green's function in the BCS pairing theory, J. Low Temp. Phys. **45**, 137 (1981).

[63] D. Kriegner, H. Reichlova, J. Grenzer, W. Schmidt, E. Ressouche, J. Godinho, T. Wagner, S. Y. Martin, A. B. Shick, V. V. Volobuev, G. Springholz, V. Holý, J. Wunderlich, T. Jungwirth, and K. Výborný, Magnetic anisotropy in antiferromagnetic hexagonal MnTe, Phys. Rev. B **96**, 214418 (2017).

[64] M. J. Grzybowski, C. Autieri, J. Domagala, C. Krasucki, A. Kaleta, S. Kret, K. Gas, M. Sawicki, R. Bożek, J. Suffczyński, and W. Pacuski, Wurtzite vs. rock-salt MnSe epitaxy: electronic and altermagnetic properties, Nanoscale **16**, 6259 (2024).

[65] T. Berlijn, P. C. Snijders, O. Delaire, H.-D. Zhou, T. A. Maier, H.-B. Cao, S.-X. Chi, M. Matsuda, Y. Wang, M. R. Koehler, P. R. C. Kent, and H. H. Weitering, Itinerant antiferromagnetism in RuO_2, Phys. Rev. Lett. **118**, 077201 (2017).

[66] G. Sarma, On the influence of a uniform exchange field acting on the spins of the conduction electrons in a superconductor, J. Phys. Chem. Solids **24**, 1029 (1963).

[67] K. Maki and T. Tsuneto, Pauli paramagnetism and superconducting state, Prog. Theor. Phys. **31**, 945 (1964).

[68] A. M. Clogston, Upper limit for the critical field in hard superconductors, Phys. Rev. Lett. **9**, 266 (1962).

[69] M. Tinkham, *Introduction to Superconductivity* (McGraw-Hill, New York, 1996).

[70] P. A. Frigeri, D. F. Agterberg, and M. Sigrist, Spin susceptibility in superconductors without inversion symmetry, New J. Phys. **6**, 115 (2004).

[71] L. P. Gor'kov and E. I. Rashba, Superconducting 2D system with lifted spin degeneracy: Mixed singlet-triplet state, Phys. Rev. Lett. **87**, 037004 (2001).

[72] T. Bernat, J. S. Meyer, and M. Houzet, Spin susceptibility of nonunitary spin-triplet superconductors, Phys. Rev. B **107**, 134520 (2023).